AIAA JOURNAL
Vol. 46, No. 9, September 2008

Technical Notes

TECHNICAL NOTES are short manuscripts describing new developments or important results of a preliminary nature. These Notes should not exceed 2500 words (where a figure or table counts as 200 words). Following informal review by the Editors, they may be published within a few months of the date of receipt. Style requirements are the same as for regular contributions (see inside back cover).

Vorticity-Preserving Artificial Dissipation Model for Vortical Wake Prediction

Chao-Ho Sung* and Bong Rhee†
David Taylor Model Basin,
West Bethesda, Maryland 20817-5700
and
T. M. Shih‡
University of Maryland, College Park, Maryland 20782

DOI: 10.2514/1.32971

Introduction

VORTICITIES shed from a bluff body normally form one or several streamwise vortical flows. These vortical flows can last for long distances downstream. Accurate prediction of these vortical flows has always been a challenge to computational fluid dynamics (CFD). The numerically predicted vorticity has the tendency to dissipate prematurely. There are several reasons for premature dissipation of the predicted vorticity in the wake: 1) numerical truncation error, 2) excessive eddy viscosity introduced by turbulence models, and 3) artificial dissipation added to maintain numerical stability for complex flows [1]. Normally, a fine grid is used in the region where vorticity is first generated, but a coarse grid is used in the wake region. The larger truncation error of the coarse grid can cause premature dissipation of the vorticity. Another way of saying this is that the grid is too coarse to resolve the vortex. Use of higher-order schemes can reduce this difficulty [2]. The excessive eddy viscosity introduced by turbulence models in the wake can be significantly reduced by detached eddy simulation, as demonstrated by Vatsa and Singer [3]. The objective of this Note is to propose an approach to overcome the third difficulty regarding the artificial dissipation already mentioned. A new vorticity-preserving artificial-dissipation model (VPAD) is developed to minimize the premature dissipation of the predicted vorticity. VPAD achieves the goal of maintaining numerical stability while minimizing the premature dissipation of vorticity.

Large eddy simulation (LES) is currently an active research topic. A survey of applications of LES to complex engineering turbulent flows has recently been presented by Fureby [4]. It appears that the capability of LES to handle massively separated flows has been demonstrated [5], but its capability to track vortical flows long distances downstream has not yet been established. However, LES does have an advantage because the eddy viscosity predicted in the wake is much smaller than that predicted by conventional turbulence models, as demonstrated in Vatsa and Singer [3]. For complex flows, Rizzetta et al. [6] observed that a certain level of artificial dissipation is needed by LES to prevent spurious numerical oscillations. Thus, LES would have the same difficulty as other methods in tracking the vertical flows long distances downstream. For this reason, VPAD should also be applicable to LES methods.

In 1994, Steinhoff [7] published a new technique called the vorticity-confinement method, which is capable of tracking vortical flows long distances downstream without premature dissipation. Many papers have been published using this technique since then (see, for example, Wenren et al. [8] and Löhner et al. [9]). The idea is simple and beautiful. In this method, a vorticity-confinement term is added to the right-hand side of the momentum equations. Anticipating premature dissipation of vorticity, the vorticity-confinement term generates new vorticity to be put back into the flow region where vorticities are generated by the flow physics. In this manner, realistic vortical flow can be simulated by a small number of grid cells and tracked for long distances downstream. Critical to this technique is the proper selection of the magnitude of the vorticity-confinement parameter that controls the amount of the new vorticity to be put back to the flow region. Unfortunately, this parameter can be determined only when the solution is more or less known and then by trial and error. It is both problem-dependent and grid-sensitive. Furthermore, the governing equations of motion have been altered because a vorticity-confinement term is added to the right-hand side of the momentum equations. It is not possible to discuss the numerical stability as a result of the addition of the vorticity-confinement term and it has not been attempted.

The new approach is inspired by Steinhoff's [7] work. The objective is to modify the artificial-dissipation model constructed by Jameson et al. [1] such that the vortices can be tracked long distances downstream. The modification is done automatically. Therefore, there is no need to select a parameter value by trial and error. In addition, because the governing equations are discretized in the conservative form with a second-order-accurate finite volume central-difference scheme and a fourth-derivative artificial dissipation, the stability of this numerical scheme will therefore be discussed.

Formulation

The formulation will be presented in a 2-D steady, inviscid, and incompressible flow. Extension to a 3-D unsteady, viscous, and incompressible or compressible flow is straightforward. Adapting an artificial compressibility model with preconditioning [10], the governing equations of motion in curvilinear coordinates ξ and η can be written as

$$\frac{\partial}{\partial t}(\mathbf{J}^{-1}q) + \frac{\partial F}{\partial \xi} + \frac{\partial G}{\partial \eta} = 0 \tag{1}$$

where t is a pseudotime, $q = (\beta^{-2}p, u, v)^t$, p is the pressure divided by the density, β^{-2} is an artificial compressibility parameter on the order of 0.7, u and v are the velocity components in the Cartesian coordinates x and y, $\mathbf{J}^{-1}$ is the transformation Jacobian that is equivalent to cell volume dV in finite volume formulation, and F and G are fluxes in the ξ and η directions, respectively.

Received 21 June 2007; revision received 28 March 2008; accepted for publication 21 April 2008.

*Senior Research Scientist, Maneuvering and Control Division; chao.sung@navy.mil.
†Research Scientist, Computational Hydrodynamics Division; bong.rhee@navy.mil.
‡Associate Professor, Department of Mechanical Engineering; tmshih@umd.edu.

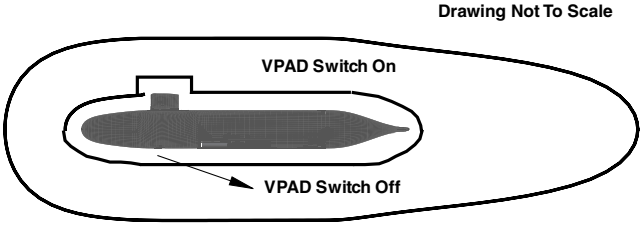

Fig. 1 A schematic drawing showing flow regions with the VPAD switch on and off around a body of revolution with a sail.

For incompressible flow, there is no shock and the second-order artificial dissipation can be neglected. Then, applying a second-order accurate central-difference spatial discretization with a fourth-derivative artificial-dissipation model and an explicit m-stage Runge–Kutta time-stepping scheme [1], the solution to Eq. (1) can be obtained as

$$\begin{gathered} q^{(0)} = q^n \\ q_{ij}^{(k)} = q_{ij}^{(0)} - \alpha_k \frac{\Delta t}{\Delta V}\left[D_\xi F_{ij}^{(k-1)} + D_\eta G_{ij}^{(k-1)} + D q_{ij}^{(k-1)} \Delta V\right] \\ k = 1, 2, \ldots, m \\ q^{n+1} = q^{(m)} \end{gathered} \tag{2}$$

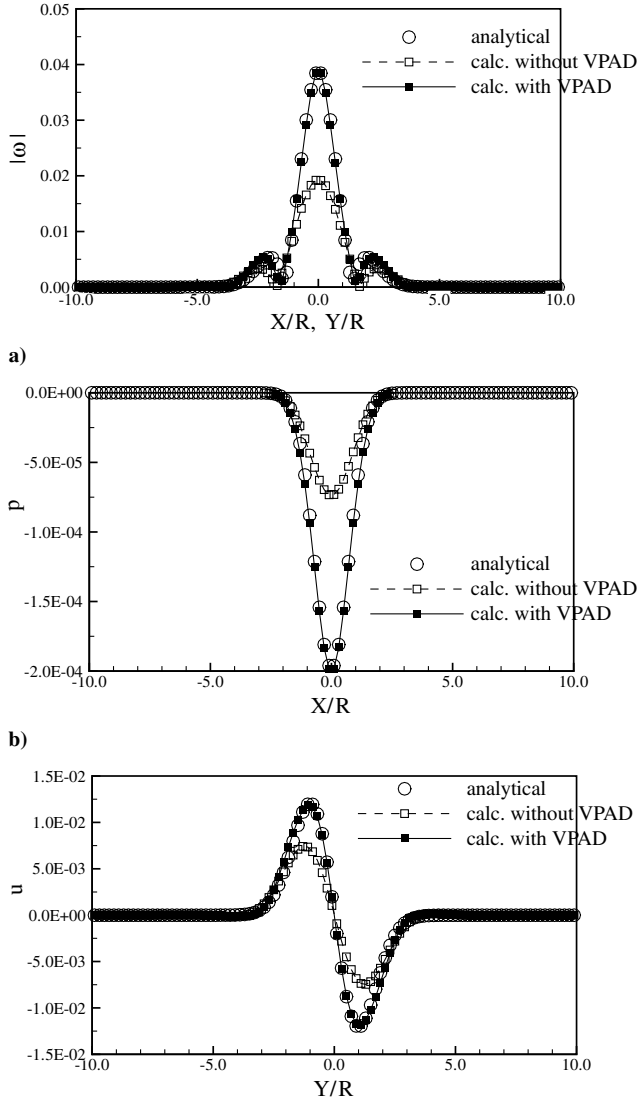

Fig. 2 Comparison of 2-D steady inviscid vortex in a box with and without VPAD after 800 multigrid cycles; artificial dissipation $\varepsilon_4 = 0.0005$ and R is the vortex core radius.

where the superscript n denotes the pseudotime level, q_{ij} is the solution vector q at point (i, j), $q^{(m)}$ is the solution at the mth stage, and α_k are the time-stepping parameters for the Runge–Kutta scheme.

$$D_\xi F_{ij}^{(k-1)} = F_{i+\frac{1}{2},j}^{(k-1)} - F_{i-\frac{1}{2},j}^{(k-1)}, \qquad D_\eta G_{ij}^{(k-1)} = G_{i,j+\frac{1}{2}}^{(k-1)} - G_{i,j-\frac{1}{2}}^{(k-1)} \tag{3}$$

$$D q_{ij}^{(k-1)} = D_\xi^4 q_{ij}^{(k-1)} + D_\eta^4 q_{ij}^{(k-1)} \tag{4}$$

$$\begin{gathered} D_\xi^4 q_{ij} = \varepsilon_4 \left(\lambda_{\xi_{i+\frac{1}{2},j}} \Delta^3 q_{i+\frac{1}{2},j} - \lambda_{\xi_{i-\frac{1}{2},j}} \Delta^3 q_{i-\frac{1}{2},j} \right) \\ \Delta^3 q_{i+\frac{1}{2},j} = q_{i+2,j} - 3q_{i+1,j} + 3q_{i,j} - q_{i-1,j} \end{gathered} \tag{5}$$

$D_\eta^4 q_{ij}^{(k-1)}$ is defined similarly, where λ_ξ and λ_η are the largest eigenvalues of the flux Jacobians F and G, respectively. The maximum eigenvalues are given as

$$\begin{gathered} \lambda^i = \tfrac{1}{2}[|U^i| + \sqrt{|U^i|^2 + 4\beta^2 |a^i|^2}], \qquad U^i = \mathbf{u} \cdot \mathbf{a}^i \\ \mathbf{a}^i = \nabla \xi^i, \qquad \xi = \xi^1 \quad \text{and} \quad \eta = \xi^2 \\ \lambda_\xi = \lambda^1 \quad \text{and} \quad \lambda_\eta = \lambda^2 \end{gathered} \tag{6}$$

The local time step is then given by

$$\Delta t < \frac{\mathrm{CFL} \Delta V}{|\lambda_\xi| + |\lambda_\eta|}, \qquad \mathrm{CFL} \sim 6.5 \tag{7}$$

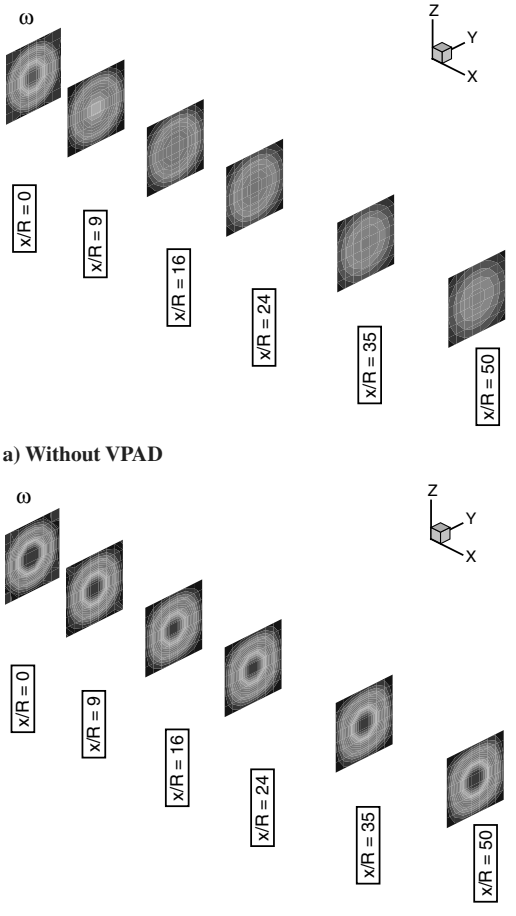

Fig. 3 Three-dimensional turbulent vortical flow in a uniform stream; $Re = 15 \times 10^6$, $\varepsilon_4 = 0.015$, k-ω turbulence model, and R is the vortex core radius.

Table 1 Comparison with experimental data

Reference	St	C_d	rms C_l
Present with VPAD	0.20	1.4	±0.63
Present without VPAD	0.19	1.37	±0.58
Williamson and Roshko [15]	0.18–0.20	——	——
Wille [16]	——	1.3	——
Norberg [17]	——	——	±0.40–0.55

The VPAD is then given as

$$q_{ij}^{(k)} = q_{ij}^{(o)} - \alpha_k \frac{\Delta t}{\Delta V}\Big[D_\xi F_{ij}^{(k-1)} + D_\eta G_{ij}^{(k-1)} + (1-\alpha_{ij}) D q_{ij}^{(k-1)} \Delta V\Big], \qquad k = 1, 2, \ldots m \tag{8}$$

where

$$\alpha_{ij} = c\frac{|\omega_{ij}|}{\max|\omega_{ij}|}, \qquad \omega = \nabla \times u \tag{9}$$

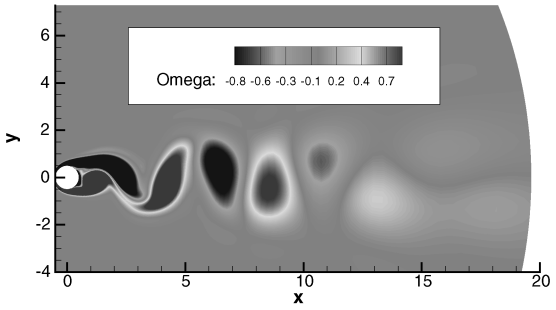

a) Vortex shedding without VPAD

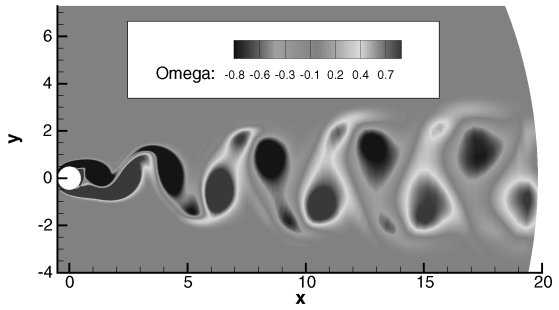

b) Vortex shedding with VPAD

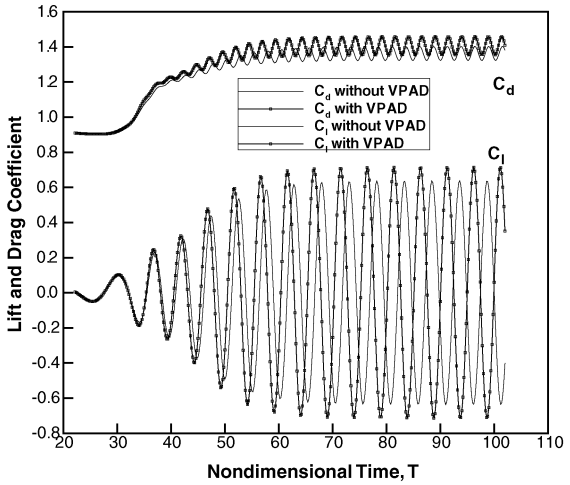

c) Time history of C_D and C_L with and without VPAD

Fig. 4 Two-dimensional unsteady laminar flow cylinder; $Re = 200$, $\varepsilon_4 = 0.0156$, and $\Delta t^* = 0.125$.

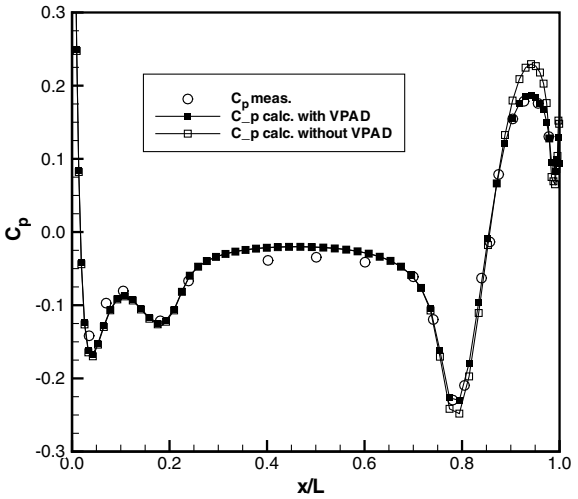

a) Pressure coefficient with and without VPAD at Re_L = 1.2x10^7, α = 0 deg, 96 x 64 x 1, 800 multigrid cycle

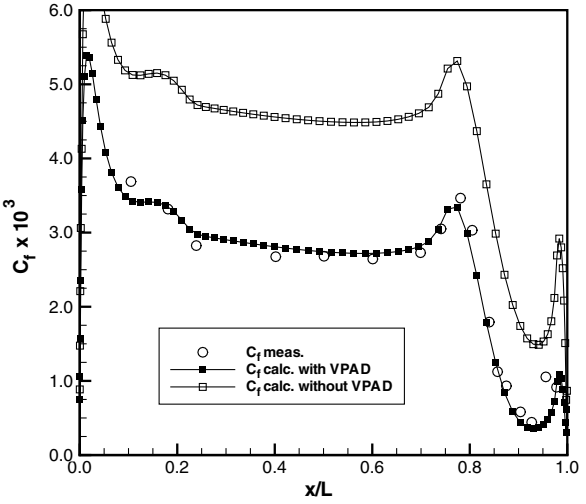

b) Skin frction coefficient with and without VPAD at Re = 1.2x10^7, α = 0 deg, 96 x 64 x 1, 800 multigrid cycle

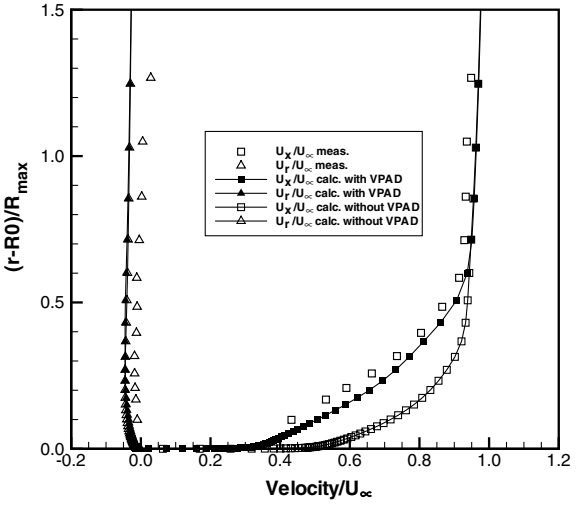

c) Velocity with and without VPAD at Re = 1.2x10^7, α = 0 deg, 96 x 64 x 1, 800 multigrid cycle

Fig. 5 Effect of VPAD on the SUBOFF bare hull.

The value of parameter c is on the order of 1 and is not very sensitive; $\alpha_{ij} = 0$ recovers the original artificial-dissipation model.

A comparison of Eqs. (2) and (8) indicates that only the artificial-dissipation term has been changed by a vorticity function α_{ij}, which is a function defined as the ratio of the absolute value of the vorticity at a local point in the computational domain and the maximum vorticity in the computational domain as given by Eq. (9). As mentioned earlier, the parameter c is on the order of 1. The vorticity function varies as the pseudotime progresses and the vorticity evolves. The vorticity function approaches zero in the flow region where the vorticity is very weak and the original artificial-dissipation model is recovered. In the flow region where the vorticity is strong, the vorticity function approaches 1 and the magnitude of the artificial dissipation is much reduced. Consequently, the vorticity is less likely to dissipate prematurely in this region.

The stability of VPAD will be succinctly described. In the absence of the viscous and artificial-dissipation terms, an explicit central-difference scheme has a small stability boundary with a Courant–Friedrichs–Lewy (CFL) number in Eq. (7) of about 1. Van der Houwen [11] developed explicit m-stage Runge–Kutta time-stepping schemes with increased stability boundaries in which the theoretical CFL number is now $\mathrm{CFL} = m - 1$, where m is the number of RK stages. These schemes have been adopted by Jameson et al. [1] and are given in Eq. (2) for a 5-stage scheme. Stability is further enhanced by implicit residual smoothing, and then a CFL number of 6.5 can be used as indicated in Eq. (7). A more detailed stability discussion of these schemes is given by Pike and Roe [12]. Although linear stability is established, nonlinear instabilities or spurious oscillations caused by shocks or, in the present case, a strong shear can still occur. Thus, a second derivative artificial dissipation (for shocks) and/or fourth-derivative artificial dissipation (for strong shear) are needed to suppress these instabilities [1]. To show that the addition of fourth-derivative artificial dissipation will not alter the stability of second-order accurate discretization scheme, it is sufficient to show that it has a stabilizing effect. Consider the following equation in one dimension:

$$\frac{\partial q}{\partial t} = -\varepsilon \frac{\partial^4 q}{\partial x^4} \tag{10}$$

where ε is a positive value. Multiplying Eq. (10) by q and then integrating by parts gives

$$\frac{1}{2}\int_v \frac{\partial q^2}{\partial t} = -\varepsilon \int_v \left(\frac{\partial^2 q}{\partial x^2}\right)^2 < 0 \tag{11}$$

Because the $q2$-norm is decreasing if the parameter ε is positive, the right-hand side of Eq. (10) is stabilizing. It follows that the fourth-derivative artificial dissipation with a proper sign and an appropriate value for ε is stabilizing. An appropriate value of ε is determined by numerical trial and error. A typical value is $1/64 = 0.0156$ [13]. Because the vorticity function α_{ij} is positive and less than 1, the modified artificial dissipation always has the same sign as the original artificial dissipation. Thus, the stability will not be altered by VPAD.

There is a restriction on the use of VPAD in turbulent boundary layers, particularly at a high Reynolds number. In this strong-shear region, the vorticity is very strong and is predominantly in the transverse direction to the flow stream. Also, in this region, where the vorticity is rapidly evolving, artificial dissipation is needed to maintain numerical stability. Applying VPAD in this region can either cause numerical instability or alter the development of flow physics. As a consequence, either the solution has the tendency to diverge or the solution is not accurate because the development of

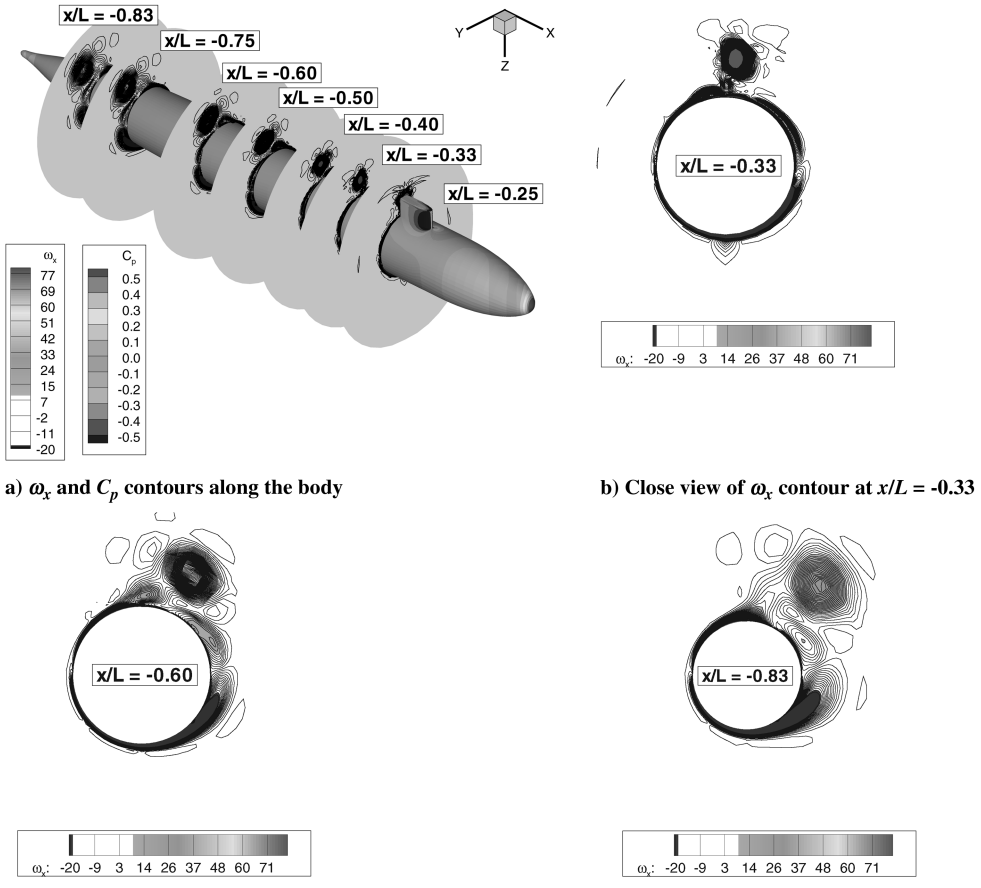

a) ω_x and C_p contours along the body

b) Close view of ω_x contour at x/L = -0.33

c) Close view of ω_x contour at x/L = -0.60

d) Close view of ω_x contour at x/L = -0.83

Fig. 6 Streamwise vorticity shed from the sail of a body of revolution and pressure contour plots without VPAD at $\beta = 6$ deg, $Re_L = 16 \times 10^6$, and $\epsilon_4 = 0.0156$ based on the straight-line basin data.

flow physics has been hindered. This will be demonstrated later. Thus, it is important to set up a criterion to determine where in the boundary layer VPAD should be switched off. A major deciding criterion is that VPAD should not interfere with the development of flow physics. Intuitively, boundary-layer thickness is a candidate. Unfortunately, the definition of boundary-layer thickness becomes ambiguous in separated flows; thus, other candidates must be considered. Define the turbulent Reynolds number:

$$R_t = \frac{k}{\nu\omega} \tag{12}$$

where k is the turbulent kinetic energy, ν is the kinematic viscosity, and ω is the specific turbulent dissipation rate. The maximum of R_t normally occurs in the log layer on the order of $y^+ \sim \mathcal{O}(10^2)$. Then the switch-off location may be defined as

$$y_{\text{switch-off}} = cR_t, \qquad c \sim 1 - 3 \tag{13}$$

The proportional factor c is problem-dependent but should be about 1 to 3. For low Reynolds number flows such as laminar flows, the switch-off of VPAD appears not important, as expected, and is demonstrated in the subsequent test cases. A schematic drawing indicating where VPAD should be switched on and where it should be switched off for a turbulent flow about a body of revolution with a sail is suggested in Fig. 1.

Description of Results

A convecting 2-D inviscid vortex investigated by Visbal and Gaitonde [14] will be considered here under a steady-state condition. This steady 2-D vortex-in-a-box problem has an analytical solution. For this simple problem, a converged solution in almost exact agreement with the analytical solution can be obtained without any addition of artificial dissipation. It will be demonstrated that even a very small amount of artificial dissipation can cause drastic diffusion of the vorticity. It will also be shown that VPAD can prevent this diffusion. A small amount of artificial dissipation with $\varepsilon_4 = 0.0005$ will be added. This value is much smaller than the typical value of $1/64 = 0.0156$ mentioned earlier. Comparisons of solutions with and without VPAD will be made after 800 multigrid cycles. The computed absolute vorticity $|\omega|$, pressure p, and x-component velocity u with and without VPAD are shown in Figs. 2a–2c, respectively. It can be seen that because much of the vorticity has been dissipated by the added artificial dissipation, peaks of absolute vorticity $|\omega|$, pressure p, and velocity u are smeared. On the other hand, when VPAD is applied, the computed results are much improved. It is interesting to note that although the fourth-derivative artificial dissipation near the vortex core is very small due to almost-rigid-body rotation of the vortex core, its effect on the vorticity is quite dramatic.

The next test case is to demonstrate that VPAD also works in a 3-D turbulent vortical flow. The same preceding vortex is released at the left boundary and propagates downstream to the right. The Reynolds number is 15×10^6, the k-ω turbulence model is used, and a typical ε_4 value of 0.0156 is used. Without VPAD, the vorticity is almost completely dissipated by the time it travels 16 vortex core radii downstream, as shown in Fig. 3a. When VPAD is applied, the vortex is only slightly dissipated at 50 vortex core radii downstream, as shown in Fig. 3b. It would be of interest to extend the outer boundary to several hundreds of vortex core radii downstream to see if VPAD still works. But because the grid rapidly becomes very coarse outward, the vorticity will disappear because of insufficient grid resolution, not because of artificial dissipation. For this reason, this exercise is not done.

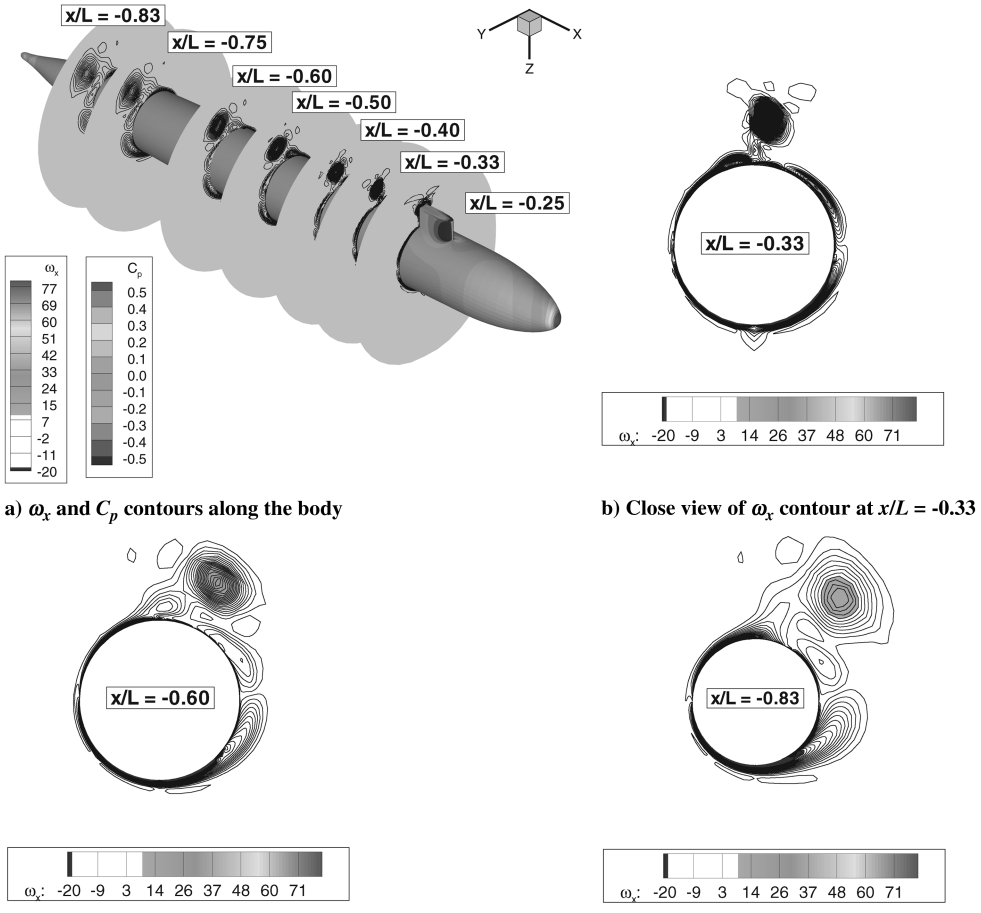

a) ω_x and C_p contours along the body

b) Close view of ω_x contour at x/L = -0.33

c) Close view of ω_x contour at x/L = -0.60

d) Close view of ω_x contour at x/L = -0.83

Fig. 7 Streamwise vorticity shed from the sail of a body of revolution and pressure contour plots with VPAD at $\beta = 6$ deg, $Re_L = 16 \times 10^6$, and $\epsilon_4 = 0.0156$ based on the straight-line basin data.

The third test case is a 2-D unsteady laminar flow over a cylinder at a Reynolds number of 200. The artificial-dissipation parameter $\varepsilon_4 = 0.0156$. The computed Strouhal number, drag, and rms lift coefficients are in good agreement with the existing experimental data, as indicated by Table 1. For a comparison with other computed results by several researchers, one is referred to Table 3 in Tai et al. [18]. The changes in the Strouhal number, drag, and rms lift coefficients with or without VPAD are insignificant, as indicated in Fig. 4c. However, the effect on the shed vortices downstream is very significant whether or not VPAD is applied, as shown in Figs. 4a and 4b. Because of the low Reynolds number, VPAD is not switched off in the boundary layer.

The fourth test case demonstrates the importance of switching off VPAD in a high Reynolds number turbulent boundary layer. A turbulent boundary-layer flow about a body of revolution called SUBOFF will be considered. The Reynolds number is 1.2×10^7 based on the body length. C_p, C_f, and the boundary-layer velocity profiles have been measured by Huang et al. [19]. The location of switch-off $y_{\text{switch-off}}$ is given by Eq. (13) with the constant $c = 2$. Figure 5a shows that the predicted C_p is about the same whether or not VPAD is switched off near the wall. The only exception is near the stern, where C_p is overpredicted without switching off VPAD. Figure 5b shows that C_f is significantly overpredicted if VPAD is not switched off near the wall, and Fig. 5c shows that the streamwise velocity component is much faster if VPAD is not switched off near the wall. All the discrepancies can be explained as follows. If VPAD is not switched off near the wall, it interferes with the development of turbulence by introducing spurious nonlinear instabilities in the local region near the wall. As a result, the turbulence is not properly developed and the boundary layer behaves more like an inviscid than a viscous flow. This explains the overprediction of C_f and u. It also explains why C_p is only overpredicted in the stern. For a well-developed turbulent boundary layer, the turbulent boundary layer becomes much thicker near the stern. But now the flow is less turbulent and more inviscid, and therefore C_p is overpredicted.

Finally, VPAD is applied to a body of revolution with a sail. The streamwise vorticity shed from a sail plays an important role in the flow physics of this type. Therefore, it is important for a numerical procedure to have the capability to track this vorticity long distances downstream. The case considered has a Reynolds number of 16×10^6 and a drift angle of 6 deg. The artificial-dissipation parameter ε_4 is 0.0156. The computed six components of forces and moments by Rhee [20] are in very good agreement with the measured data [21] whether VPAD is applied or not. However, the strength of vorticity at $x/L = 0.83$ is improved by VPAD, as indicated by comparing Figs. 6 and 7. Although VPAD does improve, it is not as significant as other test cases, for several reasons. First, it may be because of lack of grid resolution in the wake region from the sail to the stern, because only approximately one million grid cells are used in the whole computational domain. Second, the sail wake is a longitudinal vortex flow imbedded in a boundary layer where the vorticity is predominantly in the transverse direction. Therefore, it is possible that the constant parameter c in the switch-off in Eq. (13) needs to be further fine-tuned. This task will be further pursued in the future. The wake detection of a fully appended submarine in maneuver is an important problem. This type of wake is a free-shear problem in which VPAD is effective. It is speculated that VPAD may potentially be a very effective tool in wake detection. This speculation is not demonstrated because of a lack of measured data in the public domain.

Conclusions

A new vorticity-preserving artificial-dissipation model (VPAD) has been developed for the prediction of vortical wake over long distances downstream. This model is automatic in the sense that there is no need to estimate parameters by trial and error. Also, the order of VPAD is on the same order as artificial dissipation. Its accuracy, stability, and effectiveness are discussed and demonstrated by four test cases in a wide range of applications.

Acknowledgment

This work is partially funded by the In-House Laboratory Independent Research (ILIR) program at David Taylor Model Basin, monitored by John Barkyoumb. Computer resources are provided by the U.S. Department of Defense High Performance Computing Modernization Office (DOD-HPCMC) at the Naval Oceanographic Office (NAVO).

References

[1] Jameson, A., Schmidt, W., and Turkel, E., "Numerical Solutions of the Euler Equations by a Finite Volume Method Using Runge-Kutta Time-Stepping Schemes," AIAA 14th Fluid and Plasma Dynamics Conference, Palo Alto, CA, AIAA Paper 81-1259, June 1981.

[2] Abarbanel, S., and Kumar, A., "Compact High-Order Schemes for the Euler Equations," *Journal of Scientific Computing*, Vol. 3, No. 275, 1988, pp. 275–288.

[3] Vatsa, V. N., and Singer, B. A., "Evaluation of a Second-Order Accurate Navier-Stokes Code for Detached Eddy Simulation Past a Circular Cylinder," 21st AIAA Applied Aerodynamics Conference, Orlando, FL, AIAA Paper 2003-4085, June 23–26, 2003.

[4] Fureby, C., "ILES and LES of Complex Engineering Turbulent Flows," *Journal of Fluids Engineering*, Vol. 129, Dec. 2007, pp. 1514–1523.

[5] Spalart, P. R., "Strategies for Turbulence Modeling and Simulations," *International Journal of Heat and Fluid Flow*, Vol. 21, No. 3, 2000, pp. 252–263.
doi:10.1016/S0142-727X(00)00007-2

[6] Rizzetta, D. P., Visbal, M. R., and Blaisdell, G. A., "Application of High-Order Compact Difference Scheme to Large-Eddy and Direct Numerical Simulation," 30th AIAA Fluid Dynamics Conference, Norfolk, VA, AIAA Paper 99-3714, 1999.

[7] Steinhoff, J., "Vorticity Confinement: A New Technique for Computing Vortex Dominated Flows," *Frontiers of Computational Fluid Dynamics*, edited by D. A. Caughey, and M. M. Hafez, Wiley, New York, 1994.

[8] Wenren, Y., Fan, M., Wang, L., Xiao, M., and Steinhoff, J., "Application of Vorticity Confinement to Prediction of the Flow over Complex Bodies," *AIAA Journal*, Vol. 41, No. 5, May 2003, pp. 809–816.

[9] Löhner, R., Chi Yang, C., and Roger, R., "Tracking Vortices over Large Distances Using Vorticity Confinement," *24th Symposium on Naval Hydrodynamics*, Fukuoka, Japan, July 2002, pp. 950–962.

[10] Liu, C., Zheng, X., and Sung, C. H., "Preconditioned Multigrid Methods for Unsteady Incompressible Flows," *Journal of Computational Physics*, Vol. 139, No. 1, 1998, pp. 35–57.
doi:10.1006/jcph.1997.5859

[11] Van der Houwen, P. J., "Explicit Runge-Kutta Formulas with Increased Stability Boundaries," *Numerische Mathematik*, Vol. 20, No. 2, 1972, pp. 149–164.
doi:10.1007/BF01404404

[12] Pike, J., and Roe, P. L., "Accelerated Convergence of Jameson's Finite-Volume Euler Scheme Using Van Der Houwen Integrators," *Computers and Fluids*, Vol. 13, No. 2, 1985, pp. 223–236.
doi:10.1016/0045-7930(85)90027-1

[13] Turkel, E., and Vatsa, V. N., "Effect of Artificial Viscosity on Three Dimensional Flow Solutions," AIAA 21st Fluid Dynamics, Plasma Dynamics and Laser Conference, Seattle, WA, AIAA Paper 90-1444, June 1990.

[14] Visbal, M. R., and Gaitonde, D. V., "High-Order Accurate Methods for Unsteady Vortical Flows on Curvilinear Meshes," *AIAA Journal*, Vol. 37, No. 10, 1999, pp. 1231–1239.

[15] Williamson, C. H. K., and Roshko, A., "Measurements of Base Pressure in the Wake of a Cylinder at Low Reynolds Numbers," *Zeitschrift für Flugwissenschaften und Weltraumforschung*, Vol. 14, 1990, pp. 38–46.

[16] Wille, R., "Karman Vortex Street," *Advances in Applied Mechanics*, Vol. 6, Academic Press, New York, 1960, pp. 273–287.

[17] Norberg, C., "Flow Around a Circular Cylinder: Aspect of Fluctuating Lift," *Journal of Fluids and Structures*, Vol. 15, Nos. 3–4, 2001, pp. 459–469.
doi:10.1006/jfls.2000.0367

[18] Tai, C. H., Zhao, Y., and Liew, K. M., "Parallel-Multigrid Computation of Unsteady Incompressible Viscous Flows Using a Matrix-Free Implicit Method and High-Resolution Characteristic-Based Scheme," *Computer Methods in Applied Mechanics and Engineering*, Vol. 194, Nos. 36–38, 2005, pp. 3949–3983.
doi:10.1016/j.cma.2004.09.010

[19] Huang, T. T., Groves, N. C., Forlini, T. J., Blanton, J. N., and Gowing, S., "Measurements of Flows over an Axisymmetric Body with Various Appendages (DARPA SUBOFF Experiments)," *19th Symposium on Naval Hydrodynamics*, Seoul, Korea, Aug. 1992, pp. 321–346.

[20] Rhee, B., "Investigation into the Flow Field Around a Maneuvering Submarine Using a Reynolds-Averaged Navier-Stokes Code," Ph.D. Thesis, Civil Engineering, George Washington Univ., Washington, D.C., May 2008.

[21] Atsavapranee, P., Forlini, T., Furey, D., Hamilton, J., Percival, S., and Sung, C. H., "Experimental Measurements for CFD Validation of the Flow About a Submarine Model," *25th Symposium on Naval Hydrodynamics*, St. John's, Newfoundland, Canada, Aug. 2004, pp. 175–188.

X. Zhong
Associate Editor